[7]Hummel, D., "On the Vortex Formation over a Slender Wing at Large Angles of Attack," AGARD-CP-247, Oct. 1978.

[8]Pedišius, A., Janušas, V., and Zygmantas, G., "Distortion of the Structure of the Turbulent Boundary Layer by High Free-Stream Turbulence," *Fluid Mechanics Soviet Research*, Vol. 20, No. 5, 1991.

[9]White, F. M., *Viscous Flow Theory*, McGraw–Hill, New York, 1991.

[10]Baldwin, B. S., and Lomax, H., "Thin Layer Approximation and Algebraic Model for Separated Turbulent Flows," AIAA Paper 78-257, Jan. 1978.

[11]Frankel, S. H., Adumitroaie, V., Madnia, C. K., and Givi, P., "Large Eddy Simulation of Turbulent Reacting Flows by Assumed PDF Methods," *Engineering Application to Large Eddy Simulation*, FED-Vol. 162, American Society of Mechanical Engineers, 1993, pp. 81–101.

[12]Thomas, J. P., and Lan, C. E., "The Simulation and Correction of Wind Tunnel Wall Interference on Delta-Wing Lift Using Navier–Stokes and Euler Solutions," AIAA Paper 91-3300, Sept. 1991.

[13]Pollak, J., "Navier–Stokes Simulation of the Influence of Free-Stream Turbulence on the Aerodynamic Characteristics of a Delta Wing," M.S. Thesis, Univ. of Kansas, Lawrence, KS, Dec. 1993.

Transparent Acoustic Source Condition Applied to the Euler Equations

Chang-Jeon Hwang* and Duck-Joo Lee†

Korea Advanced Institute of Science and Technology, Taejon 305-701, Republic of Korea

Nomenclature

e	= total energy
$\boldsymbol{F}$	= x-direction flux vector, i.e., $[\rho u, \rho u^2 + p, \rho uv, u(e+p)]^T$
$\hat{\boldsymbol{F}}$	= ξ-direction flux vector
F_2, F_4	= related to the spatial gradient of steady flow flux in the ξ, η direction and the perturbation flux in the η direction, Ref. 1
f	= frequency
$\boldsymbol{G}$	= y-direction flux vector, i.e., $[\rho v, \rho vu, \rho v^2 + p, v(e+p)]^T$
$\hat{\boldsymbol{G}}$	= η-direction flux vector
J	= Jacobian transformation
$\hat{\boldsymbol{P}}, \hat{\boldsymbol{P}}^{-1}$	= matrix by which $\hat{\boldsymbol{U}}$ is related to $\hat{\boldsymbol{W}}$, Ref. 9
$\hat{\boldsymbol{U}}$	= conservative variable vector in the generalized coordinate system
ε	= nondimensionalized source strength
τ	= real time
τ_ξ	= time at fixed ξ

Subscripts

s	= sound source
0	= steady flow quantity

Superscripts

$'$	= perturbed quantity
$-$	= dimensional quantity

I. Introduction

RECENTLY, several investigators[1–4] have attempted to simulate acoustic problems numerically by using well-developed numerical schemes. Two approaches have been used for numerical simulations of acoustic problems. One is to use the linearized Euler equations[1,2] and the other is to use nonlinear equations[3,4] of fluid, motion, such as Euler/Navier–Stokes equations. In any approach, the appropriate solvers should be applied because the amplitude of the acoustic wave is small and most problems of aeroacoustics are fully unsteady. Consequently, a numerical solver for acoustic problems should have minimal dissipation and dispersion errors.[5] In addition, unlike the flow problems, inflow/outflow/far-field boundary conditions are critical for accurate long range simulations.[1,2,5]

Acoustic source conditions are also important in the simulation of complex acoustic phenomena, such as the reflection and transmission of an incident wave that might occur wherever there exists an area change, e.g., a rocket nozzle,[6] a muffler, or a cascade stator and rotor, etc. Thompson's idea[7] is employed for the nonreflecting boundary conditions and two kinds of acoustic source conditions, which are compatible with the nonreflecting boundary condition, are compared in this paper; one is similar to the condition implemented by Watson and Myers[1] and the other is proposed here, which also has nonreflecting properties in the source model. The source models are tested for a uniform duct with a primary source located to the right and with a secondary source located to the left.

II. Boundary and Acoustic Source Conditions

We choose the strong conservative form of two-dimensional Euler equations of inviscid gas dynamics as governing equations. Conventional numerical schemes for the Euler equations are employed, using an upwind finite difference formulation[8] and Runge–Kutta time stepping.[9] The numerical flux is based on Roe's approximate Riemann solver with an entropy fix.[8] Higher order schemes can be constructed from MUSCL.[8] In addition, the slope limiter function, called Koren's differentiable limiter, is used to prevent the numerical solution from oscillations.[8] Based on this numerical scheme for the governing equations, the nonreflecting boundary condition and the two source conditions are described.

A. Nonreflecting Boundary Conditions

First we will briefly describe Thompson's boundary condition,[7] which is closely related to the acoustic source condition to be described later. At the inlet or outlet boundary of $\xi = \text{const}$ as shown in Fig. 1, the wave can be considered as one dimensional so that

$$\partial_{\tau_\xi} \hat{\boldsymbol{U}} + \partial_\xi \hat{\boldsymbol{F}} = 0 \tag{1}$$

Then, using Eq. (1), we can rewrite the two-dimensional Euler equations at the ξ boundary as[7]

$$\partial_\tau \hat{\boldsymbol{U}} + \partial_\eta \hat{\boldsymbol{G}} = -\partial_\xi \hat{\boldsymbol{F}} = \partial_{\tau_\xi} \hat{\boldsymbol{U}} \tag{2}$$

where

$$\hat{\boldsymbol{U}} = (\rho, \rho u, \rho v, e)^T / J$$

$$\hat{\boldsymbol{F}} = (\xi_x \boldsymbol{F} + \xi_y \boldsymbol{G}) / J$$

$$\hat{\boldsymbol{G}} = (\eta_x \boldsymbol{F} + \eta_y \boldsymbol{G}) / J$$

We must evaluate the terms $\partial \hat{\boldsymbol{U}} / \partial \tau_\xi$ in order to integrate in time at the boundaries. The terms $\partial \hat{\boldsymbol{U}} / \partial \tau_\xi$ can be obtained from Eq. (1) by diagonalizing the flux Jacobian matrix $\hat{\boldsymbol{A}} = \partial \hat{\boldsymbol{F}} / \partial \hat{\boldsymbol{U}}$ as

$$\partial_{\tau_\xi} \hat{\boldsymbol{W}} + \hat{\Lambda} \partial_\xi \hat{\boldsymbol{W}} = 0 \tag{3}$$

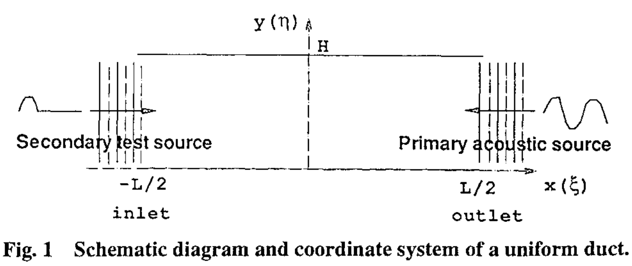

Fig. 1 Schematic diagram and coordinate system of a uniform duct.

Received Nov. 20, 1994; revision received March 20, 1995; accepted for publication April 17, 1995.

*Graduate Student, Department of Aerospace Engineering. 373-1, Kusong-dong, Yusong-gu.

†Associate Professor, Department of Aerospace Engineering, 373-1, Kusong-dong, Yusong-gu. Member AIAA.

where

$$\delta\hat{U} = \hat{P}\,\delta\hat{W}$$

$$\partial\hat{W} = (\partial W_1, \partial W_2, \partial W_{3,4})^T = \left(\delta\rho - \delta p/c^2, \delta q_t, \delta p \pm \rho c\,\delta q_n\right)^T$$

$$\hat{\Lambda} = \mathrm{diag}\,(\lambda_1, \lambda_2, \lambda_{3,4}) = \mathrm{diag}\,(q_n, q_n, q_n \pm c)$$

$$q_n = \hat{\xi}_x u + \hat{\xi}_y v, \qquad q_t = \hat{\xi}_y u - \hat{\xi}_x v$$

$$\hat{\xi}_x = \xi_x \Big/ \sqrt{\xi_x^2 + \xi_y^2}, \qquad \text{etc.}$$

Equation (3) can be decomposed into incoming and outgoing parts based on the directions of the eigenvalue λ_1,

$$\partial_{\tau_\xi}\hat{W}|_{\rm in} + \hat{\Lambda}|_{\rm in}\partial_\xi\hat{W} = 0, \qquad \partial_{\tau_\xi}\hat{W}|_{\rm out} + \hat{\Lambda}|_{\rm out}\partial_\xi\hat{W} = 0 \tag{4}$$

For example, the eigenvalues λ_1, λ_2, and λ_3 correspond to the incoming part and λ_4, to the outgoing part at the inlet. To be a nonreflecting boundary,[10] $\hat{\Lambda}|_{\rm in}$ is set to zero. Thus, the values of incoming characteristic variables remain unchanged at the boundaries. Therefore, we can rewrite Eq. (4) as

$$\partial_{\tau_\xi}\hat{W}|_{\rm in} = 0, \qquad \partial_{\tau_\xi}\hat{W}|_{\rm out} = -\hat{\Lambda}|_{\rm out}\,\partial_\xi\hat{W} \tag{5}$$

In Eq. (5), $\hat{\Lambda}|_{\rm out}(\partial\hat{W}/\partial\xi)$ are calculated by one-sided difference. Then, the terms $\partial\rho/\partial\tau_\xi$, $\partial p/\partial\tau_\xi$, $\partial q_n/\partial\tau_\xi$, and $\partial q_t/\partial_{\tau_\xi}$ in $\partial\hat{U}/\partial\tau_\xi$ in Eqs. (2) are obtained by solving Eqs. (5) simultaneously. Then Eqs. (2) are integrated in time along with the interior values.

B. Acoustic Source Conditions

Now consider the acoustic source condition, which can be also considered as an incoming wave. The term, $\partial\hat{W}/\partial\tau_\xi|_{\rm in}$ in Eq. (4) should be specified by appropriate relations to make the incoming wave equivalent to a sound source. First, we use the linear plane wave relations,[10] which are valid in stationary or uniformly moving medium, where + is right going and − is left going,

$$\begin{aligned} \partial_{\tau_\xi} p &= \varepsilon\omega\cos(\omega\tau) \\ \partial_{\tau_\xi} q_n &= \pm\partial_{\tau_\xi} p/\rho c \\ \partial_{\tau_\xi} q_t = 0, &\qquad \partial_{\tau_\xi}\rho = \partial_{\tau_\xi} p/c^2 \end{aligned} \tag{6}$$

At the inlet, Eq. (5) can be rewritten as

$$\left\{\begin{array}{c} \partial_{\tau_\xi} W_1|_{\rm in} = \partial_{\tau_\xi}\rho - \partial_{\tau_\xi} p/c^2 = 0 \\ \partial_{\tau_\xi} W_2|_{\rm in} = \partial_{\tau_\xi} q_t = 0 \\ \partial_{\tau_\xi} W_3|_{\rm in} = \partial_{\tau_\xi} p + \rho c\partial_{\tau_\xi} q_n \neq 0 \end{array}\right\}, \qquad \partial_{\tau_\xi} W_4|_{\rm out} = -\lambda_4\partial_\xi W_4 \tag{7}$$

At the outlet,

$$\begin{aligned} \partial_{\tau_\xi} W_l|_{\rm out} &= -\lambda_1\partial_\xi W_l \qquad (l = 1, 2, 3) \\ \partial_{\tau_\xi} W_4|_{\rm in} &= \partial_{\tau_\xi} p - \rho c\partial_{\tau_\xi} q_n \neq 0 \end{aligned} \tag{8}$$

These source conditions are specified as a transparent source in this paper, which permits the nonreflecting property at the boundary on the source side.

Other acoustic source conditions have been used by Watson and Myers.[1] They decompose the fluid variables into a steady flow and an acoustic perturbation component as

$$\hat{W} = \hat{W}_0 + \hat{W}' \tag{9}$$

In their paper, the unknown $\partial\hat{W}'/\partial\tau_\xi$ in the Eq. (4) is written in terms of their notation b_{1s}, b_{2s}, b_{3s}, and b_{4s} where

$$\left\{\begin{array}{l} \partial_{\tau_\xi} W_1' = -\lambda_1\partial_\xi W_1' = \lambda_1 b_{1s}/c^2 \\ \partial_{\tau_\xi} W_l' = -\lambda_l\partial_\xi W_l' = \lambda_l b_{ls} \qquad (l = 2, 3, 4) \end{array}\right\} \tag{10}$$

which are related to $\partial\hat{W}'/\partial\xi$.

For the case of source excited at the outlet, the outgoing wave is related to b_{1s}, b_{2s}, and b_{3s} and the incoming wave is related to b_{4s} only. The terms b_{1s}, b_{2s}, and b_{3s} are calculated by one-sided difference, and b_{4s} is obtained with the outgoing wave component b_{3s} and the specified source quantity p_s' as follows:

$$\begin{aligned} b_{4s} &= [2(\partial_t p_s' + F_4) - \lambda_3 b_{3s}]/\lambda_4 \\ p_s' &= \varepsilon\sin(\omega t) \end{aligned} \tag{11}$$

The inlet source condition, which is derived here, can be described as follows by using the isentropic relation and the zero vorticity condition:

$$\begin{aligned} b_{1s} &= b_{2s} = 0 \\ b_{3s} &= [2\rho c(\partial_t u_s' + F_2) + \lambda_4 b_{4s}]/\lambda_3 \\ u_s' &= \varepsilon\sin(\omega t) \end{aligned} \tag{12}$$

and b_{4s} is calculated using one-sided differencing. These inlet/ outlet source conditions are called the Watson–Myers' source in this paper. For this type of source, the nonreflecting property on the source side is not satisfied because the specified acoustic source propagating to the interior domain is related to the outgoing wave components b_{3s} and b_{4s} for the outlet and the inlet source cases, respectively, in Eqs. (11) and (12).

III. Results and Discussion

The length and time scales are nondimensionalized by the duct height $\tilde{H}$ and $\tilde{H}/\tilde{c}_0$, respectively, where $\tilde{c}_0$ is the speed of sound in the flow at rest. The density and the pressure are nondimensionalized by the quantities in the flow at rest. The velocity is nondimensionalized by the speed of sound. Tests are carried out in a uniform duct as shown in Fig. 1, where $L = 3$ and $H = 1$. The time step $\Delta\tau = 0.0025$ and $f = 1$. At the outlet ($x = L/2$), two kinds of primary source conditions described in the preceding section, i.e., transparent source and Watson–Myers' source conditions, are continuously excited for each case using the following relation:

$$\partial_\tau p' = \varepsilon\omega\cos(\omega\tau) \tag{13}$$

where $\omega = 2\pi f$. A wavelet is generated at the inlet ($x = -L/2$) to find the nonreflecting property on the primary source side located at the outlet as follows:

$$\partial_\tau p' = \begin{cases} \varepsilon\omega\cos(\omega\tau) & \text{if } 0 \le \omega\tau \le \pi \\ 0 & \text{otherwise} \end{cases} \tag{14}$$

A grid system, which is 181 × 15 in the ξ and η directions, is used, and the space is discretized by uniform meshes. The source amplitude ε is 0.001, which is within the linear range.

In Fig. 2a, the isolines of the perturbed pressure are shown. The secondary wavelet generated at the inlet collides with the outlet boundary at $t = 3$. On the left side of Fig. 2a, i.e., the case of Watson–Myers' primary source, the wavelet is reflected by the outlet source, which is described with dense contour lines. As shown on the right side of Fig. 2a, however, the wavelet generated at the inlet propagates without reflection when the transparent source proposed in this paper is excited at the outlet and the interior field is not contaminated by the reflected wavelet. Figure 2b show these facts quantitatively. For the case of Watson–Myers' primary source, the reflection is detected at $t = 5$ with a large negative peak value in the time histories. This is a natural result of the formulation for the transparent source condition. The Watson–Myers' source represents a physically existing source, such as a speaker at the boundary, and so the wavelet is reflected at the boundary. The transparent source model is useful for simulating the acoustic source numerically in

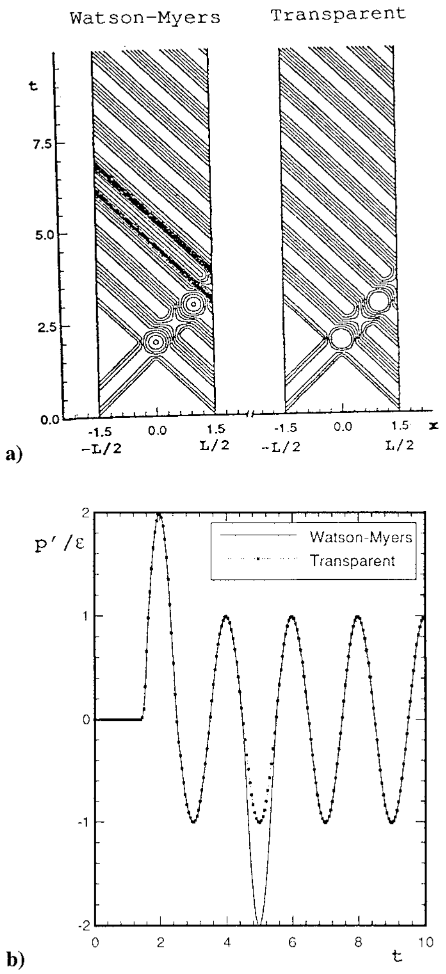

Fig. 2 Tests of nonreflecting property for sound source side at outlet by a wavelet generated at inlet, $M_\infty = 0$: a) x–t diagrams of $p'/\varepsilon, y = H/2$ and b) time histories, $x = 0, y = H/2$.

the computational domain when the actual source is located far downstream.

IV. Conclusion

It can be concluded from the present calculations that the transparent source model proposed here is useful to numerically simulate an acoustic source in the computational domain that is located far downstream. Thus, it is possible to simulate a complex acoustic problem, such as the reflection and transmission of an incident wave. On the other hand, the Watson–Myers' source is a physically existing source, such as a speaker at the boundary. Therefore, care should be taken when choosing acoustic source conditions as well as nonreflecting boundary conditions.

References

[1]Watson, W. R., and Myers, M. K., "Inflow-Outflow Boundary Conditions for Two-Dimensional Acoustic Waves in Channels with Flow," *AIAA Journal*, Vol. 29, No. 9, 1991, pp. 1383–1389

[2]Lee, D. J., and Koo, S. O., "Numerical Study of Sound Generation Due to a Spinning Vortex Pair," AIAA Paper 93-4370, Oct. 1993.

[3]Meadows, K. R., Caughey, D. A., and Casper, J., "Computing Unsteady Shock Waves for Aeroacoustic Applications," AIAA Paper 93-4329, Oct. 1993.

[4]Lele, S. K., "Compact Finite Difference Schemes with Spectral-like Resolution," *Journal of Computational Physics*, Vol. 103, 1992, pp. 16–42.

[5]Roe, P. L., "Technical Prospects for Computational Aeroacoustics," DGLR/AIAA Paper 92-02-032, May 1992.

[6]Bolcs, A., Frasson, T. H., and Platzer, M. F., "Numerical Simulation of Inviscid Transonic Flow Through Nozzles With Fluctuating Back Pressure," *Journal of Turbomachinery*, Vol. 111, April 1989, pp. 169–180.

[7]Thompson, K. W., "Time Dependent Boundary Conditions for Hyperbolic Systems," *Journal of Computational Physics*, Vol. 68, 1987, pp. 1–24.

[8]Yee, H. C., "A Class of High-Resolution Explicit and Implicit Shock-Capturing Methods," NASA TM 101088, Feb. 1989.

[9]Hirsch, C., *Numerical Computation of Internal and External Flows*, 1st ed., Vol. 2, Wiley, New York, 1990, pp. 183, 408–594.

[10]Dowling, A. P., and Ffowcs Williams, J. E., *Sound and Sources of Sound*, 1st ed., Ellis Horwood, West Sussex, England, UK, 1983, pp. 65–69.

Nonequilibrium Anisotropic Eddy–Viscosity/Diffusivity Turbulence Model for Heated Turbulent Flows

Wenyan Ni,* John G. Kawall,† and James F. Keffer‡

University of Toronto, Toronto, Ontario M5S 1A4, Canada

Introduction

In general, there are two types of turbulence models in use, viz; 1) the standard eddy–viscosity/diffusivity (SEV) model and 2) the Reynolds stress/flux (RS) model.

The SEV model is relatively simple and effective; in addition, it is easy to incorporate into most turbulence computational fluid dynamics (CFD) computer codes. However, it has three major deficiencies: 1) It is subject to the assumption that all normal Reynolds stresses are essentially equal (the isotropic assumption). 2) It is subject to the assumption of local equilibrium, which implies that the eddy–viscosity coefficient is a constant throughout the whole field. 3) It does not account for the effect of buoyancy explicitly.

In contrast, the RS model can account for buoyancy effects, as well as the anisotropy and nonequilibrium properties of turbulence. But, this model (even in its algebraic form) is computationally less efficient than the SEV model and is often numerically unstable.[1]

Because of the deficiencies of the SEV model just noted, considerable research effort has been directed toward the development of a nonlinear eddy–viscosity model.[2] However, these models do not deal with thermal turbulence quantities and do not account for buoyancy effects.

In the present study, a nonequilibrium anisotropic form of the eddy–viscosity/diffusivity turbulence (NAEV) model has been developed for heated turbulent flows. The NAEV model is designed to deal with both the Reynolds stresses and Reynolds heat fluxes with the advantages of numerical efficiency and stability.

Derivation of the Nonequilibrium Anisotropic Eddy–Viscosity Model

The NAEV model is derived from the algebraic second-moment (ASM) model which has the following complete form for determining the Reynolds stresses ($-\overline{u_iu_j}$) and heat fluxes ($-\overline{u_i\theta}$) (see Refs. 2 and 3):

$$-\overline{u_iu_j} = -\tfrac{2}{3}k\delta_{ij} + 2f_\mu c'_{\mu0}(k^2/\varepsilon)S_{ij} - (k/\varepsilon)f_\mu\Big[\alpha_1\big(P_{ij} - \tfrac{2}{3}P\delta_{ij}\big) + \alpha_2\big(C_{ij} - \tfrac{2}{3}P\delta_{ij}\big) + \alpha_3\big(G_{ij} - \tfrac{2}{3}G\delta_{ij}\big)\Big] \tag{1}$$

$$-\overline{u_i\theta} = \frac{k}{\varepsilon}f_t\left[\alpha_{t1}\overline{u_iu_j}\frac{\partial T}{\partial x_j} + \alpha_{t2}\overline{u_j\theta}\frac{\partial U_i}{\partial x_j} + \alpha_{t3}\beta g_i\overline{\theta^2}\right] \tag{2}$$

In these two equations, k and ε are the turbulence kinetic energy

Received Sept. 1, 1994; revision received Nov. 22, 1994; accepted for publication Dec. 3, 1994.

*Research Assistant, Department of Mechanical Engineering. Member AIAA.

†Associate Professor, Department of Mechanical Engineering.

‡Professor, Department of Mechanical Engineering.